

ISSN 1989-9572

DOI: 10.47750/jett.2022.13.05.055

Investigation of Standardized Moments of Force Distribution in Simple Liquids

**1Dr.SHAFEE UR RAHAMAN MOHMAD,
2Mr.SANTHOSH THOTA**

Journal for Educators, Teachers and Trainers, Vol.13 (5)

<https://jett.labosfor.com/>

Date of Reception: 12 July 2022

Date of Revision: 13 Aug 2022

Date of Acceptance: 20 September 2022

Dr.SHAFEE UR RAHAMAN MOHMAD, Mr.SANTHOSH THOTA (2022). Investigation of Standardized Moments of Force Distribution in Simple Liquids. Journal for Educators, Teachers and Trainers, Vol.13(5). 592-599.

Investigation of Standardized Moments of Force Distribution in Simple Liquids

1Dr.SHAFEE UR RAHAMAN MOHMAD,2Mr.SANTHOSH THOTA

12Assistant Professor

DEPT of H&S

Vaagdevi College of Engineering, Warangal, TS, India

ABSTRACT

This study investigates the standardized moments of force distribution in simple liquids, aiming to provide a comprehensive understanding of their physical properties and behavior under various conditions. By employing analytical and computational methods, we analyze how different factors, such as temperature, viscosity, and molecular interactions, influence the distribution of forces within these liquids. Our findings reveal key insights into the relationship between molecular dynamics and macroscopic properties, enhancing the understanding of fluid behavior in both theoretical and practical applications. This research contributes to the broader field of fluid mechanics and offers valuable information for the design and optimization of liquid-based systems.

1 INTRODUCTION:

We can better fit coarser models that recreate these 1–3 by knowing the moments and measures of a distribution for a fully atomistic molecular dynamics (MD) simulation. In model coarse graining, it is often the case that we want to immediately reconcile the completely atomistic system's energy landscape to a simpler representation that preserves as many of the system's physical characteristics as feasible at the lowest possible computing cost. However, it is also normal to try to replicate the force distribution that would naturally result in the energy landscape 5–10 by matching forces between the high and low resolution systems. Let $F = [F_1, F_2, F_3]$ represent a force acting on a liquid's tagged atom. Force F may fluctuate across a range of values depending on the relative locations of other atoms. In this book, we will refer to this as the force distribution. By computing the features of its equilibrium distribution, we can acquire extensive information about F . Every force coordinate has the same equilibrium distribution when an isotropic system is taken into consideration. By averaging over the k -th power of its initial coordinate, we get the standardised moment of the force distribution as

$$\alpha_k = \frac{\langle F_1^k \rangle}{\langle F_1^2 \rangle^{k/2}}, \quad (1)$$

where F_1^k is the k -th moment of the force distribution and α_k standardises the k -th moment by scaling it with the k -th power of the standard deviation of the force distribution. In a simple homogeneous fluid with radially symmetric interactions between particles, the force distribution will exhibit symmetry around the origin and thus all odd standardised moments vanish, i.e. $0 = \alpha_1 = \alpha_3 = \alpha_5 = \dots$. As $\alpha_2 \equiv 1$ by definition (1), the first non-trivial standardised moment is kurtosis, denoted α_4 , which provides a measure of spread that details how tailed the force distribution is relative to a normal distribution [1]. In this paper, we study how the force distribution depends on the number density of a homogeneous many-body system, and the temperature of the same system in a canonical ensemble. We will do this by studying the behaviour of the second moment of the force distribution F_1^2 and standardised even moments $\alpha_4, \alpha_6, \alpha_8, \dots$. If the force distribution was Gaussian, then the even standardised moments would be

$$\alpha_k = (k-1)!! = \prod_{i=1}^{k/2} (2i-1), \quad \text{for } k = 2, 4, 6, 8, 10, \dots, \quad (2)$$

and the second moment F_1^2 would be sufficient to parametrize the force distribution. However, the force distributions in simple liquids have been reported to deviate from Gaussian distribution [2–14]. In particular, by

comparing the results of our analysis with Gaussian moments in equation (2), we can also quantify how non-Gaussian the real force distribution is.

Much work has been done in the area of force distributions of many-body systems: with seminal work from Chandrasekhar¹⁵ that employed Markov's theory of random flights to give an expression for the force distribution of a many-body system interacting through a $1/r$ gravitational potential. More recent work has been done with the help of MD by Gabrielliet al¹⁶, who derived an expression for the kurtosis of the force distribution for a lattice system of atoms interacting through the gravitational potential. Further, using the classical density functional theory, an expression for the probability distribution of force for a system interacting through an arbitrary weakly repulsive potential was derived by Rickayzen et al^{17,18}.

In this paper, we study the number density and temperature dependence of the force distribution for a many-body system interacting through a Lennard-Jones 12-6 potential^{19,20}, which is ubiquitously used and has been shown to model homogeneous systems of interacting (Argon) atoms well^{21–23}.

The simple two-body system in one spatial dimension is thoroughly examined in Section III, which offers the perfect setting for demonstrating the fundamental techniques while maintaining intriguing dynamical behaviour. basic-order partial differential equations (PDEs) that describe the dependency of the standardised moments of the force distribution on parameters are derived from basic principles. By doing this, we also get an analytical equation for the partition function of a two-body system that is precise in an asymptotic limit of the density going to zero ($n \rightarrow 0$) and that relies only on the standardised moments of the force distribution. The temperature-dependent PDE is also used to develop a formula that links the system's average energy to standardised moments of force. We determine the leading order behaviour of the kurtosis of the force distribution in the limit $n \rightarrow 0$ using a truncated Taylor series expansion in parameter regimes where long-range interactions between atoms predominate. Lastly, we determine the leading order behaviour of the standardised moments of force at low temperatures ($T \rightarrow 0$) using a Laplace integral approximation. The effectiveness of these techniques and underlying presumptions are shown by the results of a basic MD simulation. The inevitable conclusion that asymptotic behaviour is determined by long-range force computations is then extended from the 1D model to many-body systems of any size in three spatial dimensions in Section IV. These systems include periodic boundary conditions using the minimal image convention and cubic geometry, which are the physical characteristics of typical MD simulations.

II. NOTATION

We consider a system of N identical atoms interacting via the Lennard-Jones 12-6 potential¹⁹. This is a ubiquitous interatomic pairwise potential; here the potential between atoms labelled $i, j = 1, 2, \dots, N$ positioned at $\mathbf{q}_i, \mathbf{q}_j \in \mathbb{R}^3$ is given (in reduced units²⁴) by the expression

$$U_{ij}(r_{ij}) = 4 \left(\frac{1}{r_{ij}^{12}} - \frac{1}{r_{ij}^6} \right), \quad (3)$$

where $r_{ij} = |\mathbf{q}_i - \mathbf{q}_j|$ is the distance between atoms. The Lennard-Jones potential (3) between two atoms has a unique minima obtained at $r_{ij} = r_* = 2^{1/6}$.

We employ the framework of statistical mechanics for this closed many-body system and describe atom $i = 1, 2, \dots, N$ by phase space coordinates $\{\mathbf{q}_i, \mathbf{p}_i\} \in \mathbb{R}^6$, where \mathbf{p}_i denotes the momentum of the i -th atom. We work in the canonical ensemble with temperature T ; the partition function therefore becomes

$$\mathcal{Z}_N(T, V) = \frac{1}{h^{3N} N!} \int_{\Omega_{\mathbf{q}} \times \Omega_{\mathbf{p}}} \exp[-\beta H(\mathbf{q}, \mathbf{p})] d^3 \mathbf{q} d^3 \mathbf{p}, \quad (4)$$

where V is the volume of our closed system, and $\mathbf{q} = (q_1, q_2, \dots, q_N)$ and $\mathbf{p} = (p_1, p_2, \dots, p_N)$ are vectors containing the positions and momenta of all atoms in the system. Our integration domain is given by $\Omega_{\mathbf{q}} \times \Omega_{\mathbf{p}} \subset \mathbb{R}^{3N} \times \mathbb{R}^{3N}$. This denotes the phase space of our system. For systems of interest $\Omega_{\mathbf{p}} \equiv \mathbb{R}^{3N}$. The underlying geometry of the system (and principle simulation cell) is a cubic box of size $L > 0$, therefore $\Omega_{\mathbf{q}} \equiv (-L/2, L/2] \times \dots \times (-L/2, L/2]$. The phase space volume elements in equation (4) are denoted by

$$d^3 \mathbf{q} = \prod_{i=1}^N d^3 \mathbf{q}_i \quad \text{and} \quad d^3 \mathbf{p} = \prod_{i=1}^N d^3 \mathbf{p}_i. \quad (5)$$

Throughout this work we make use of reduced units²⁴, utilising Argon parameters²⁵. In particular, all instances of T in this work can be translated back to SI units with the transformation $T \rightarrow k_B T$ where k_B is the Boltzmann factor. Therefore, in the partition function (4), we have $\beta = 1/T$ and h is the Planck constant (≈ 0.186 in reduced units). Finally, $H(\mathbf{q}, \mathbf{p})$ is the classical Hamiltonian $H(\mathbf{q}, \mathbf{p}) = K(\mathbf{p}) + U(\mathbf{q})$ with kinetic energy $K(\mathbf{p}) = |\mathbf{p}|^2/2$ (where

the usual factor of mass is unity under reduced units) and a general potential $U(q)$. The statistical average of a quantity X for this N -body system is given by

$$\langle X \rangle = \frac{1}{\mathcal{Z}_N h^{3N} N!} \iint_{\Omega_q \times \Omega_p} X \exp[-\beta H(\mathbf{q}, \mathbf{p})] d^3 \mathbf{q} d^3 \mathbf{p}, \quad (6)$$

where the Boltzmann factor acts as a statistical weighting for a configuration $\{\mathbf{q}, \mathbf{p}\} \in \mathbb{R}^{6N}$, normalised such that $h^3 = 1$. We label atoms so that the first one is the tagged atom. Denoting the force on the tagged atom produced from the j -th atom by $\mathbf{F}_j = [F_{j,1}, F_{j,2}, F_{j,3}] \in \mathbb{R}^3$, for $j = 2, 3, \dots, N$, the total force $\mathbf{F} = [F_1, F_2, F_3]$ on the tagged atom is

$$\mathbf{F} = \sum_{j=2}^N \mathbf{F}_j.$$

We define

$$f_k = \int_{\Omega_q} \left(\sum_{j=2}^N F_{j,1} \right)^k \exp[-\beta U(\mathbf{q})] d^3 \mathbf{q} \quad (7)$$

for $k = 0, 1, 2, \dots$. Then we have

$$\frac{f_k}{f_0} = \left\langle \left(\sum_{j=2}^N F_{j,1} \right)^k \right\rangle = \langle F_1^k \rangle.$$

Then the k -th standardised moment (1) is given by

$$\alpha_k = \frac{f_0^{k/2-1} f_k}{f_2^{k/2}}, \quad (8)$$

where we are interested in cases $k = 4, 6, 8, \dots$

In order to study how the force distribution depends on the physical parameters of interest it is useful to identify how changes in these parameters will manifest themselves in the system. Indeed, we choose to work in the canonical ensemble with a target temperature of T : this is accomplished with the use of a thermostat which is discussed further in Section IV B and Appendix B. It is more illuminating to see that if we have a system with a fixed number of free interacting atoms N in a cubic box of side L ; the (reduced) number density is given by $n = N/L^3$. Therefore the approach we employ in this paper to ascertain how values of standardised moments depend on number density, will be to keep the number of atoms fixed but vary the box width L - this will manifest as a change in density n . Similarly one could keep the volume of the cubic box the same and vary the number of atoms though this is a point of discussion in Section IV B.

For the remainder of the paper we will study systems with different spatial dimensions. The size of the system varies by changing the number of particles N ; we will use equation (8) as a crucial initial point in each calculation. We will naturally proceed by investigating systems of increasing complexity; starting from a cartoon one-dimensional model and culminating to a general many-body system of arbitrary size in three spatial dimensions.

III. ONE ATOM IN A POTENTIAL WELL

We now go on to illustrate three approaches to obtain the dependence of the force distribution on parameters n and T . It is useful to note that, as we are now working in one spatial dimension, density n is proportional to $1/L$, i.e. we have $n \propto 1/L$. We will consider a simple system in one spatial dimension consisting of two atoms interacting through the Lennard-Jones potential (3) in interval $[0, L]$ with periodic boundary conditions. One of the atoms is considered to be fixed at position $q_0 = L/2 \in [0, L]$ and the other atom is free to move, therefore, we have $N = 1$ free atom. Its position is denoted $x \in [0, L]$. Therefore, the inter-atomic distance is $r = |x - q_0|$. Using our simplified one-dimensional set up, $F_1 = F$ and $\Omega_q = (0, L)$, equation (7) reduces to

$$f_k(L) = \int_0^L F^k(|x - q_0|) \exp[-\beta U(|x - q_0|)] dx, \quad (9)$$

which is the marginalised expected value of the k -th moment of force $F(x) = -dU/dx$, where we have dropped subscripts in the Lennard-Jones potential (3) and we write it as $U(z) = 4(z^{-12} - z^{-6})$. Utilising the symmetry of the potential (and therefore the force) we are left with

$$f_k(L) = 2 \int_0^{L/2} F^k(r) \exp[-\beta U(r)] dr. \quad (10)$$

In what follows, we will assume that we are in a regime where the box width L satisfies $L \gg r^*$, where $r^* = 2/6$ minimizes the Lennard-Jones potential U .

A. Differential equation for standardised moments

We consider a perturbation of the form $L \rightarrow L + \delta L$. Using equation (10) and considering terms to the order $O(\delta L)$, we obtain

$$\begin{aligned} f_k(L + \delta L) &= f_k(L) + f'_k(L) \delta L + O(\delta L^2) \\ &= f_k(L) + F^k(L/2) \exp[-\beta U(L/2)] \delta L + O(\delta L^2). \end{aligned}$$

Using equation (8), we approximate $\alpha_k(L + \delta L)$

$$\alpha_k(L) + \alpha_k(L) v_k(L) \exp[-\beta U(L/2)] \delta L + O(\delta L^2),$$

where our notation $\alpha_k(L)$ highlights the dependence of the standardised moments of force, α_k , on L , and function $v_k(L)$ is given

$$v_k(L) = \frac{k-2}{2f_0(L)} + \frac{F^k(L/2)}{f_k(L)} - \frac{kF^2(L/2)}{2f_2(L)}. \quad (11)$$

Taking the limit $\delta L \rightarrow 0$, we obtain the derivative of the k -th standardised moment of force, with respect to L ,

$$\frac{\partial \alpha_k}{\partial L}(L) = v_k(L) \exp[-\beta U(L/2)] \alpha_k(L), \quad (12)$$

where $v_k(L)$ are expressed in terms of integrals (10) as given by equation (11).

B. Far-field integral approximation

To further analyze integrals (10), we introduce a cutoff c , which satisfies that $r^* < c < L/2$, where $r^* = 2/6$ is a unique maximum of $\exp[-\beta U(z)]$, which can be Taylor expanded as $\beta(1 + 4z - 6 + 4z - 12 - 16/3z - 18 + 8z - 24 \dots)$. Considering sufficiently large L , we can choose the cutoff c , so that

$$\left| f_0(L) - 2 \left(\int_0^c \exp[-\beta U(r)] dr + \beta \int_c^{L/2} 1 + \frac{4}{r^6} dr \right) \right| \leq \varepsilon, \quad (13)$$

where tolerance ε is chosen to be 10^{-4} in our illustrative computations. This splitting allows us to numerically calculate the bulk of the integral (10) as a constant independent of L and then use the second term to give an analytic expression for α_k with dependence on L , and ultimately on n .

The range of values of T that are of typical use are chosen in order to maintain the liquid state of Argon during simulation. These are approximately temperatures in the interval $0.70 < T < 0.73$ under ambient conditions²⁶. Therefore, as volume is varied we are in a regime where $\beta = O(1)$, for convenience we set $\beta = 1$. Though given that the density of our system changes between each simulation some systems will be in a liquid phase and others in a gaseous phase, this is a point of discussion in Section IV B.

Splitting the integration domain $[0, L/2]$ of integral (10) into $[0, c]$ and $[c, L/2]$, we use the exact form of the integrand in $[0, c]$ to obtain a 'near-field' contribution. Utilising an approximate form for the integrand given by the truncated Taylor expansion $f(z)$ in the domain $[c, L/2]$ gives rise to a density dependent 'far-field' contribution. Combining these we arrive at the approximate form for $f_0(L)$. Using cutoff $c = 2$, equation (13) is satisfied with $\varepsilon = 10^{-4}$. Therefore, upon numerically calculating the bulk contribution for the integral with domain $[0, 2]$, we get

$$f_0(L) = 2 \int_0^{L/2} \exp[-\beta U(r)] dr = b_0 + L + O(L^{-6}) \quad (14)$$

$$\frac{\partial \alpha_k^0}{\partial L}(L) = \frac{k-2}{2(b_0 + L)} \alpha_k^0(L).$$

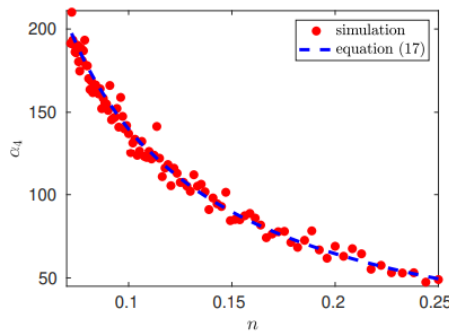


FIG. 1. Plot of α_4 as a function of $n = 1/L$ for the illustrative one-atom system. Results of MD simulations are compared with $\alpha_4 = -10.828 + 15.074n - 1$ obtained by using equation (17) with b_0 , b_2 and b_4 given by (16) (blue dashed line). MD simulation results for temperature $T = 1$ utilising Langevin dynamics²⁷ described in equation (B1), with friction parameter $\gamma = 0.1$, are represented by red dots. The MD simulation length was a total of 1.1×10^8 time steps with the first 107 time steps used for initialisation.

Finally this gives us tha

$$\mathcal{Z}_1(T, V) = \frac{1}{h} \int_0^L \exp[-\beta U(q)] dq \int_{-\infty}^{\infty} \exp\left[-\frac{\beta p^2}{2}\right] dp, \quad (20)$$

where the Planck factor of $1/h$ arises instead of $1/h^3$ due to the fact that we are in one-dimensional physical space. Using (10), we obtain

$$f_0(L) = h \mathcal{Z}_1(T, V) \sqrt{\frac{\beta}{2\pi}}. \quad (21)$$

Considering the low density limit $n \rightarrow 0$ (i.e. $L \rightarrow \infty$) in equation (12) and using (18) and (21), we obtain

$$\mathcal{Z}_1(T, V) \sim \frac{(k-2)\sqrt{2\pi}}{\sqrt{h^2\beta}} \left[\alpha_k(L) \left(\frac{\partial \alpha_k}{\partial L}(L) \right)^{-1} \right], \quad (22)$$

as $L \rightarrow \infty$. In particular, we can obtain the partition function (20) in the dilute (low density) limit by using information

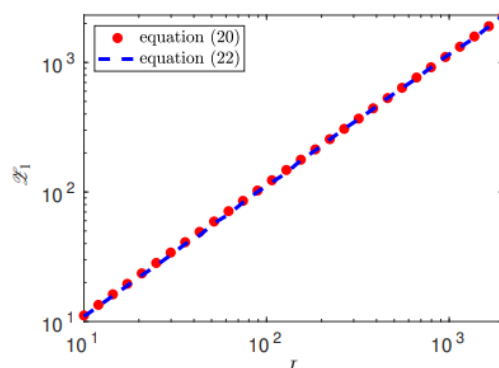


FIG. 2. Approximation of the partition function $\mathcal{Z}_1(T, V)$ obtained using the right hand side of equation (22) with $k = 4$ and values of kurtosis (α_4) estimated from MD simulation (blue dashed line). The exact values obtained by (20) are plotted as the red dots.

about the moments of the force distribution. The accuracy of equation (22) is illustrated in Figure 2, where we use $k = 4$. We use MD simulations of a single atom, using a range of simulation box widths L . We estimate the values of kurtosis of the force distribution, its derivative with respect of L and use the right hand side of equation (22) to estimate the $\mathcal{Z}_1(T, V)$. Considering $L \geq 10$, the result is within 5% error when compared with the exact result (20), while for larger values of box width L the error decreases to around 1%, confirming that the formula (22) is valid in the asymptotic limit $L \rightarrow \infty$.

C. Temperature dependence of standardised moments

One can perform a similar analysis as in Section III A, viewing the moments $\alpha_k = \alpha_k(T)$ as a function of temperature $T = 1/\beta$. To do that, we consider the moment definition (10) as a function of temperature T , namely, we define

$$f_k(T) = 2 \int_0^{L/2} F^k(r) \exp\left[-\frac{U(r)}{T}\right] dr. \quad (23)$$

Considering small perturbations of these functions with respect to $T \rightarrow T + \delta T$, while fixing the domain length L , and collecting terms up to first order in δT , we obtain

$$\frac{\partial \alpha_k}{\partial T}(T) = v_k(T) \alpha_k(T), \quad (24)$$

Where

$$v_k(T) = \left(\frac{k}{2} - 1\right) \frac{f'_0(T)}{f_0(T)} + \frac{f'_k(T)}{f_k(T)} - \left(\frac{k}{2}\right) \frac{f'_2(T)}{f_2(T)}. \quad (25)$$

Combining equations (24) and (25) with equation (21) where $\beta = 1/T$, we obtain

$$\frac{\partial}{\partial T} \ln\left(\frac{\alpha_k^2 f_2^k}{f_k^2}\right) = (k-2) \left(\frac{\partial}{\partial T} \ln(\mathcal{Z}_1) - \frac{1}{2T}\right).$$

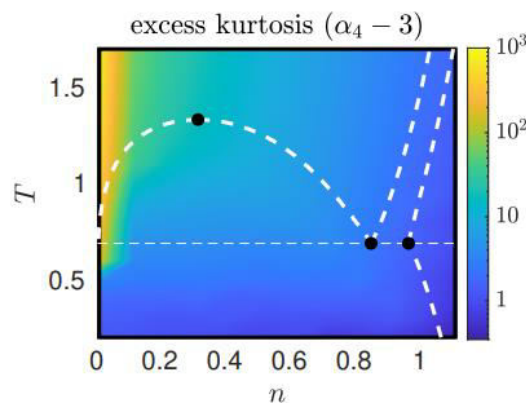
Since $-\partial/\partial\beta(\ln\mathcal{Z}_1)$ is equal to the average energy of the system, $\langle E \rangle$, we have

$$\langle E \rangle = \frac{T}{2} + \frac{T^2}{k-2} \frac{\partial}{\partial T} \ln\left(\frac{\alpha_k^2 f_2^k}{f_k^2}\right), \quad (26)$$

V. DISCUSSION AND CONCLUSIONS

We have shown in Section III that a range of techniques may be used to investigate the temperature and number density dependence of the standardised moments of the force distribution. This gives rise to a rich structure in which we demonstrate that these standardised moments may be used to compute the partition function for a 1D system in its entirety. Section IV examines the relationship between α_k and number density n by applying the far field technique presented in Section III B to a system with N atoms in three-dimensional physical space.

For $n < 1.11$ and $T \leq 1.7$, the excess kurtosis, $\alpha_4 - 3$, is computed as a function of temperature T and density n . The coexistence lines of several phases of a Lennard-Jones fluid are shown by the white dotted lines, which are derived from the literature 32–35. The critical point and the vapour-liquid-solid triple points are shown by the solid black dots (left to right), which yields the asymptotic equation (38). MD simulations of four systems of $N = 2, 8, 64, 512$ interacting Lennard-Jones atoms are compared with our analytical findings. Although the findings for systems with greater values of N are shown to converge more rapidly to the theoretically anticipated outcomes, the results nonetheless show good agreement with theoretical expectations. Specifically, systems with lower values of N lack rich dynamics like clustering of Lennard-Jones fluids entirely, whereas systems with N as tiny as $N = 64$ atoms catch these dynamics. Because atoms are energetic and may push closer together to experience greater forces, α_k generally increases as temperature rises. Clustering at the vapour-liquid coexistence phase causes a bifurcation point, as shown in Figure 6, where a significant increase in the standardised moments of force is observed. However, regardless of the temperature/number density domain under study, a general increase in temperature or a decrease in number density causes an increase in α_4 , as shown in Figure .



REFERENCES

1. S. Joshi and S. Deshmukh, A review of advancements in coarsegrained molecular dynamics simulations. Molecular Simulation, DOI: 10.1080/08927022.2020.1828583 (2020)

2. Y. Wang et al. Effective force coarse-graining. *Physical Chemistry Chemical Physics* 11, p2002 (2009)
3. R. Erban and S. J. Chapman. *Stochastic modelling of reaction-diffusion processes*, Cambridge Texts in Applied Mathematics, Cambridge University Press (2020)
4. H. Ingólfsson et al. The power of coarse graining in biomolecular simulations. *Wiley Interdisciplinary Reviews: Computational Molecular Science* 4(3), p225 (2014)
5. A. Davtyan et al. Dynamic force matching: A method for constructing dynamical coarse-grained models with realistic time dependence. *Journal of Chemical Physics* 142, 154104 (2015)
6. R. Erban. Coupling all-atom molecular dynamics simulations of ions in water with Brownian dynamics. *Proceedings of the Royal Society A* 472(2186):20150556 (2016)
7. D. Wales. Exploring energy landscapes. *Annual Review of Physical Chemistry* 69, p401 (2018)
8. R. Gunaratne et al. On short-range and long-range interactions in multiresolution dimer models. *Interface Focus* (3), rsfs.2018.0070 (2019) 9E. Rolls, Y. Togashi and R. Erban. Varying the resolution of the Rouse model on temporal and spatial scales: application to multiscale modelling of DNA dynamics. *Multiscale Modeling and Simulation* 15(4), p1672 (2017)
10. R. Erban. From molecular dynamics to Brownian dynamics, *Proceedings of the Royal Society A* 470(2167): 20140036 (2014)
11. L. DeCarlo. On the meaning and use of kurtosis. *Psychological Methods* 2(3), p292 (2014)
12. A. Carof, R. Vuilleumier and B. Rotenberg. Two algorithms to compute projected correlation functions in molecular dynamics simulations. *Journal of Chemical Physics* 140, 124103 (2014)
13. H. Shin et al. Brownian motion from molecular dynamics. *Chemical Physics* 375, p316 (2010)
14. R. Erban. Coarse-graining molecular dynamics: stochastic models with non-Gaussian force distributions. *Journal of Mathematical Biology* 80, p457 (2020)
15. S. Chandrasekhar. Stochastic problems in physics and astronomy. *Review of Modern Physics* 15:1 (1943)
16. A. Gabrielli et al. Force distribution in a randomly perturbed lattice of identical atoms with $1/r^2$ pair interaction. *Physical Review E* 74:021110 (2006)
17. G. Rickayzen et al. Single atom force distributions in simple fluids. *Journal of Chemical Physics* 137, 094505 (2012)
18. A. C. Branka, D. M. Heyes and G. Rickayzen. Pair force distributions in simple fluids. *Journal of Chemical Physics* 135, 164507 (2011)
19. J. Jones. On the determination of molecular fields. — II. From the equation of state of a gas. *Proceedings of the Royal Society A*, 106:738 (1924)
20. H. Watanabe, N. Ito and C. Hu. Phase diagram and universality of the Lennard-Jones gas-liquid system. *Journal of Chemical Physics* 136, 204102 (2012)